The Thesis Committee for Gregory Nicholas Arcangeli
Certifies that this is the approved version of the following thesis:

Influence of Slat-type Blinds on Energy Consumption in Office Buildings

APPROVED BY
SUPERVISING COMMITTEE:

Supervisor:

Atila Novoselac

Matthew L Fajkus

Influence of Slat-type Blinds on Energy Consumption in Office Buildings

by

Gregory Nicholas Arcangeli, B.A., M.Arch.

Thesis

Presented to the Faculty of the Graduate School of

The University of Texas at Austin

in Partial Fulfillment

of the Requirements

for the Degree of

Master of Science in Engineering

The University of Texas at Austin

August 2012

Acknowledgements

Thanks to Dr. Atila Novoselac for his exceptional support and guidance, both during this project and in related pursuits. He is a rare combination of a top-notch research scientist and an excellent instructor and advisor. Thanks to Assistant Professor of Architecture Matt Fajkus for serving as a reader and for supporting this research in his role as Director of the UT Thermal Lab.

Doctoral candidate Steven Bourne was very generous with his time, even in the face of approaching qualifying exams. He helped me resolve several problems in the experimental set-up, and even brought cookies, coffee, and "humor" to our meetings.

Thanks to Dason Whitsett for his advice, and for putting me through solar geometry boot camp.

Jeff McCord cleared the lab schedule and kept intruders off the experiment deck, and Jae-hong Koh and Myriam Arcangeli got up early to help with physical lab set-up.

Abstract

Influence of Slat-type Blinds on Energy Consumption in Office Buildings

Gregory Nicholas Arcangeli, M.S.E.

The University of Texas at Austin, 2012

Supervisor: Atila Novoselac

Highly glazed facades of commercial buildings are desirable from the point of view of architects, building owners, and building occupants because they create visual connections with the outdoors, offer the possibility for a naturally-lit workplace, and satisfy certain aesthetic desires. The physical properties of glass, however—even when part of the best current window systems—means that this form of environmental separation is highly vulnerable to thermal flux from and to the outdoor environment. The transmission of solar radiation to the perimeter spaces represents an important source of thermal influx, and is typically controlled with shading devices. At best, shading devices create a secondary thermal barrier between indoor and outdoor environments, which can lower energy consumption, decrease peak load, allow for smaller HVAC systems, and provide better occupant comfort. The physical influence of indoor blinds, though, is not always so straightforward. They tend to create two primary effects that operate in opposing directions in regards to energy consumption: (1) they reflect a portion of shortwave solar radiation entering the building back to the outdoors, and (2) they

significantly increase the window surface area available for convective heat transfer, which can increase the convective fraction of solar gain, and potentially increase the magnitude of the instantaneous cooling load. For these reasons, the overall impact of interior blinds on equipment load and energy consumption is difficult to foresee. This study describes the results of experiments that tested various configurations of blinds in an outdoor test chamber that simulates conditions in a highly-glazed commercial office building. A simulation model that gives good agreement with experimental results was simultaneously developed. This model will allow retroactive parametric testing of blind parameters for the same given weather and internal load conditions.

Table of Contents

List of Tables

List of Figures

Chapter 1: Introduction

Buildings account for just over 40% of the energy consumed in the United States. Roughly 12.5% of this building energy—5% of the U.S. net total—is directly attributable to windows, and windows' connection with lighting means that they influence another 5% of the country's expenditures. In other words, estimated window-related energy use totals nearly 9 quads per year; equal to the annual equivalent consumption of all US passenger vehicles. Clearly, the potential for saving energy in this sector is enormous.

The largely glazed facades of typical commercial buildings affect heat transfer between the indoor and outdoor environments in several ways, including the transmission of solar radiation and the rate of heat conduction through the façade. In addition, the amount of useable daylight transmitted through the façade can affect the energy consumption of artificial lighting systems. As such, the current generation of glazed facades represents a major source of energy consumption, while offering the possibility for energy savings through design improvements.

In many commercial buildings, solar radiation is usually controlled with shading devices. These devices range from complex computer controlled layered louvers and screens, to fixed exterior fins or shelves, and simple interior blinds. All of these devices can reduce cooling energy consumption by reducing the flux of energy from the outdoor environment to the internal space, and can also be used to mediate daylighting and reduce use of indoor lighting. Proper design and operation of these devices can contribute to lower energy consumption, peak load reduction, downsized equipment, and increased comfort. The thermal effects of shading devices are thus incredibly important to the

calculation of convective and radiative heat fluxes into the building and need to be included in the calculation of various energy efficiency analyses and design procedures.

A trend in commercial buildings is the creation of increasingly complex glazed facades driven by difficult-to-balance desires of maximizing views and daylighting, while minimizing detrimental environmental thermal loads. Such systems are characterized by multi-layer assemblies that may include several lites of glass with varying properties, gas layers, and shading devices such as blinds, shades or screens which may be controlled by an automated building management system. For all of their positive potential, it is important to recognize that both the solar and heat transfer interactions present in complex fenestration systems with shading devices are complex and multi-faceted. Consider two facts regarding the presence of a shading layer, discussed by Wright et. al.,: 1) A shading layer generally reduces solar gain, but 2) a shading layer located on the indoor side of the window increases (roughly triples) the surface area available for convective heat transfer, increasing the convective fraction of the solar gain in most cases and potentially increasing immediate cooling load. Since these effects operate in opposite directions, the overall impact on equipment load and energy consumption is difficult to foresee.[1]

While considering the topic of model validation it should be recognized that the development of models and software regarding shading devices is at an early stage. Various organizations (e.g., TNO in the Netherlands, LBNL in the US, the Fraunhoffer Institute in Germany, Lund University in Sweden) have recognized the potential for operable shading devices and have taken an active interest in creating computer models for window shading attachments. Each has made progress but none has established a

[1] 2009. Wright et. al. ASHRAE RP-1311, *Improving Load Calculations for Fenestration with Shading Devices*

comprehensive set of models as each organization works to further develop this new technology. Similarly, few "real world" experimental measurements have been made. Currently there is no clear, comprehensive benchmark against which new shading attachment models can be judged.

This paper describes experiments which directly measure the effect of venetian blinds (adjustable slat-type blinds) on cooling energy within office buildings with large glazing fractions. The experiments were performed within a dedicated full-scale façade testing facility which is exposed to real weather conditions. The effect of venetian blinds with various positions relative to the glazing layers, different slat angles, and material properties were investigated. Numerical models were developed in parallel using EnergyPlus whole-building modeling software, and validated using the experimental measurements of daily cooling energy. The models could then be used to retroactively estimate the performance of alternate shading configurations for the weather conditions on the day of the original experiment. In the following sections, this paper provides a summary of similar published research, describes the experimental setup and the experimental matrix, and provides results and analysis of the findings.

Chapter 2: Literature Review

There is a considerable body of recent published research that explores the topic of blinds in complex fenestration systems. Papers tend to fall into a few broad categories: the effect of blinds on day lighting, the effects of blinds on heat transfer through the building envelope, or the effect of blinds on thermal comfort of occupants. Many of these studies employ simulation software to test, for example, the effect of slat angle control strategies on day lighting and heating and cooling energy. However, a few use data from reduced-scale experiments using solar simulators or small environmental chambers. The number of studies employing full-scale well-controlled experiments under real weather conditions is surprisingly small.

The recent study of relevance is ASHRAE RP-1311, *Improving Load Calculations for Fenestration with Shading Devices* (Wright et. al., 2009), and several associated papers by the same authors. The goal of the project was to improve the accuracy of building energy modeling software for complex window assemblies that include blinds, screens, or shades. The model developed by the research team extends existing methods for tracking radiative flux through multi-layer fenestration via a radiosity method, but with an expanded set of eleven solar properties at each layer. It also calculates energy transfer due to convection at each layer of the glazing and shade system. A thermal resistance model for a venetian blind in a glazing cavity was formulated with heat transfer measurements and confirmed by various means including the use of computational fluid dynamics (CFD). Experimental validation of the models was performed mainly at the level of sub-components: physical properties of the shading elements were measured with various techniques (BAI-IS, guarded heater plate,

spectrophotometer). Validation of the models for the full-multi-layer window systems was performed at an indoor solar simulator. The authors found good correlation with the solar transmission model for blinds, but noted that the outdoor side convection coefficient is likely a mild, but still important factor that affects the solar heat gain coefficient (SHGC) of window assemblies, and could not captured in their indoor experiments.

Lomanowski and Wright (2007) presented a heat transfer analysis of windows with venetian blinds. A coupled radiation-convection simulation method based on a model developed by Kotey and Wright (2006) was used to examine the effects of position of blinds relative to the glazing (inside. between, outside) and the color of the blinds (light or dark). The authors point out that an interior venetian blind increases the surface area of the window assembly available to participate in convective transfer to the room—the glazing surface, and each side of the blinds are involved. They found that in the case of a dark-colored indoor-side blind, the combined radiative and convective heat gains can become large enough to completely offset any decrease in solar transmission due to the blinds. In effect the blinds do nothing to reduce solar gain, and can in fact increase the peak-cooling load when used in large thermal mass constructions, since energy from radiation and convection is delivered to the room without any time lag. Other findings were that exterior blinds reduce net heat gain to the indoor space much more than interior blinds, and also that when there is no solar radiation (night) blind position also affects the rate of heat loss from the room.

Tzempelikos and Athienitis (2006) examined window shading design strategies in terms of their impact on cooling and lighting energy loads. They focus on time-based control strategies of a roller blind via transmittance schedules in order to minimize energy for heating, cooling, and lighting. Simulations were carried out in custom software and in EnergyPlus, which was used to calculate interior convection. The

findings point to the added effectiveness of automated control for blinds, and that optimal control strategies vary based on window orientation, climate, and the particular load profile of a building.

Loutzenhiser et al. (2008) performed an empirical validation of the different window solar gain models used by EnergyPlus, DOE-2.1E, and IDA-ICE. Overall performance was assessed by comparing cooling power used in the experiments with that predicted by the software. Experiments were conducted during the summer in an outdoor room-scale testing chamber in Duebendorf, Switzerland, meant to simulate a typical office. No shading devices were used with the glazing assembly; the study's focus was on an accounting of complex frame and edge effects, which are typically modeled in simulation software in a simplified fashion using empirical coefficients. Statistical analyses and comparisons were used to account for experimental uncertainties and software input uncertainties. Findings indicated a reasonable correlation between the experiment and models, showing an absolute average difference of 5.8% for EnergyPlus, 9.9% for DOE-2.1E, and 6% for IDA-ICE.

In a parallel study, Loutzenhiser et al. (2007) performed an experimental validation of a glazing unit with exterior and interior blind assemblies. Reflective exterior blinds were tested at 0-degrees and 45-degrees, and interior mini-blinds were tested at the same angles. A case with no blinds was not tested, and therefore blind effectiveness is not reported, since the study's goal was merely to validate simulation software methods for modeling fenestration with blinds. The authors use statistical method to relate the hourly uncertainties to experimental measurements with those inherent in the EnergyPlus model. EnergyPlus was found to fall within the credible limit, and the mean percentage of the absolute mean differences for EnergyPlus was 6.1 %

Gomes et al. (2012) published a study of a numerical and empirical study of the optical properties of venetian blinds. It provides an overview of the current standard models for predicting solar transmittance through blinds, including 2D raytracing and the net radiation method employed by EnergyPlus, and by the authors of ASHRAE RP-1311. They note variations in the net radiation method, which differ primarily in the method of slat discretization, and propose their own variant of this method after performing sensitivity testing of several slat discretization models. Their optimized model showed very close agreement with the current EnergyPlus model. Experimental tests of an outdoor blind mounted over a single pane of glass in an office building showed good agreement for total solar transmittance when both direct and diffuse radiation were present (i.e., during the morning), but some differences for diffuse solar transmittances in the afternoon. These differences were deemed to be in an acceptable range (find actual figures).

Chantrasrisalai and Fisher (2004) compared current slat blind models used in energy modeling software. They concluded that there is no significant difference between the models when calculating total cooling energy. Shortcomings were identified in all of the models, however. In the case of the EnergyPlus model developed by Simmler, Fischer and Winkelmann, the model's lack of correct for slat curvature can, in certain cases, substantially over-predict the direct-to-direct transmittance for curved-slat blinds.

Chapter 3: Objectives

Findings from ASHRAE RP-1311, "Improving Cooling Load Calculations for Fenestration with Shading Devices," indicate that shading devices are generally beneficial for reducing loads, but the study also demonstrated a counter-example. When dark colored venetian blinds were modeled at the interior surface of the window, they showed potentially harmful effects by rapidly releasing solar thermal energy to the room air via convection, thus increasing peak load. Since the accurate modeling of glazed facades is crucial to load calculations and energy analyses, this proposed research aims to build on the work of RP-1311.

The contribution of this paper is the experimental examination of the multi-modal heat transfer mechanisms present in office spaces glazing with shading systems under "real world" conditions. Six experiments investigate the performance of a curtain wall facade system with different shading configurations and the resultant cooling load in a prototypical office space. The goals of the experiments are to:

- Quantitatively examine the effect on the magnitude cooling load of various shading configurations
- Quantitatively examine the effect on the time of peak load for different shading configurations
- Quantitatively characterize the effect on cooling load profiles of properties of the shading devices (e.g. position in the facade assembly, reflectivity, and slat angle)

Chapter 4: Methodology

The experimental portion of this study was conducted in the UT Thermal Lab at the Center for Sustainable Development (CSD) within the University of Texas School of Architecture (UTSoA). [2] This chapter describes the, experimental setup used, the methods employed in the experiments, and the method used for the formulation of the experimental results.

UT THERMAL LAB

Experiments were conducted in the UT Thermal Lab. The Lab is designed to represent a single office space on the perimeter of a typical mid-size commercial office building. The chamber is located outdoors on steel deck 6 meters above street level. All exterior surfaces of the lab are completely exposed to outdoor weather conditions. Five of the lab's six sides (ceiling, floor, and 3 walls) are heavily insulated, to minimize heat transfer from the surroundings. The fourth wall represents the building façade, which can be modified or replaced in order to test façade design strategies. The heavy insulation of the other surfaces accomplishes two goals. First, it simplifies the task of measuring the performance of the façade. Second, it simulates typical office building conditions with the assumption that temperatures of neighboring offices and corridor are nearly identical, so that practically all of the thermal loads within the office can be attributed to the performance of the façade and any internal equipment and occupancy loads normally found in an office space.

[2] See http://soa.utexas.edu/csd/research/experimental-research/

Figure 4.1: UT Thermal Lab (top) and modeled geometry of the chamber.

The lab is located in Austin, Texas at lat. 30.28522, long. 97.740688 and is 183 meters above sea level. The exterior "façade" of the lab faces 4° west of solar south.

The interior space of the lab is 3.62 meters wide (east to west), 3.98 m deep (south to north) and 2.82 m tall. The modifiable south façade insert is 3.58 m wide and 2.64 m tall. The construction assembly for the insulated walls, ceiling, and floor is shown in the tables below. The average U-value for these walls was determined through testing to be 0.1067 W/m^2K.

Surface	Material	Thickness [m]
Walls and ceiling	Gypsum drywall	0.032
	Fiberglass-reinforced polyisocyanurate	0.11
	Structural insulated panel (SIP)	0.102
	Cementious panel over air gap	0.013
Floor	Gray carpet	0.003
	Plywood	0.038
	Fiberglass-reinforced polyisocyanurate	0.11
	Structural insulated panel (SIP)	0.102

Table 4.1: Layers of Thermal Lab insulated assembly. Layers for each wall are listed in order from interior to exterior.

The south-facing wall contains the façade insert, which is made of glazing within thermally-broken aluminum frame and dividers in a typical curtain wall assembly. The

windows are sourced from the manufacturer PPG, and consist of two layers of 6 millimeter glazing with a 13-millimeter argon-filled gap. The back side of the exterior glazing layer has a low-emissivity coating designed to reduce transmission of shortwave solar radiation. The inner glass pane is clear. Properties for the window glass were obtained from the International Glazing Database (IGDB) maintained by Lawrence Berkeley National Laboratory (LBNL). The faced insert has 3 such windows, separated by vertical dividers.

Layer	Property [units]	Value
Exterior glass (Viracon, Low-E)	Thickness [m]	0.0057
	τ_solar at normal incidence	0.386
	ρ_solar, front, at normal incidence	0.272
	ρ_solar, back, at normal incidence	0.455
	τ_visible at normal incidence	0.79
	ρ_visible, front, at normal incidence	0.059
	ρ_visible, back, at normal incidence	0.049
	τ_infrared, normal incidence	0
	ε_infrared hemispherical, front	0.84
	ε_infrared hemispherical, back	0.035
	Conductivity [W/mK]	1
Interior glass (clear)	Thickness [m]	0.0057
	τsolar at normal incidence	0.77
	ρ_solar, front, at normal incidence	0.072
	ρ_solar, back, at normal incidence	0.073
	T_visible at normal incidence	0.886
	ρ_visible, front, at normal incidence	0.085
	ρ_visible, back, at normal incidence	0.085
	τ_infrared, normal incidence	0
	ε_infrared hemispherical, front	0.84
	ε_infrared hemispherical, back	0.84
	Conductivity [W/mK]	1

Table 4.2: Glazing properties. τ= transmittance, ρ= reflectance, ε= emissivity

Calculation of Cooling Energy

The cooling system for the lab consists of a chiller with a cooling capacity of 5275 W (1.5 ton, 18000 Btu/h), which cools a loop of single-phase chilled water-ethylene glycol mix (22.8% ethylene glycol). One hundred percent return air is circulated within the lab fan coil unit at a constant rate over a cooling coil to provide cooling.

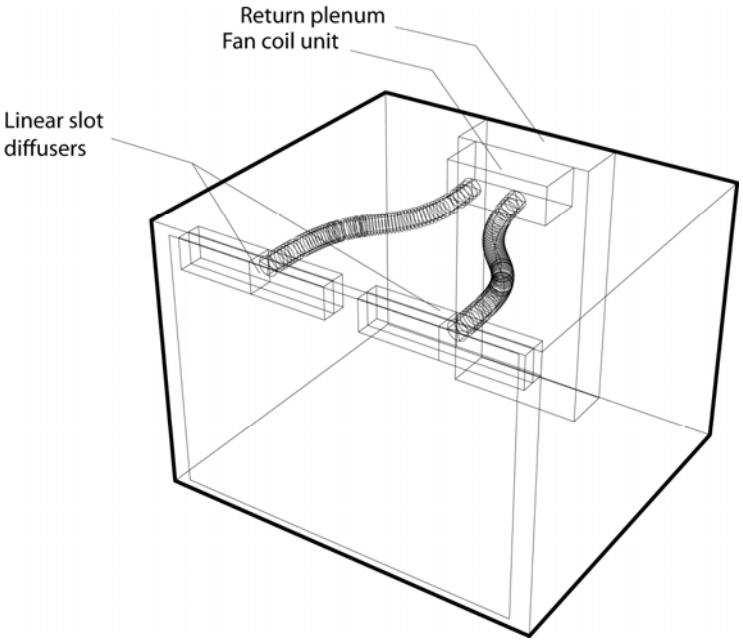

Figure 4.2: Cooling system schematic diagram

Temperatures are monitored on the chiller loop entering and leaving the cooling coil. A flow meter measures the volumetric flow rate in the chiller loop. The properties of the water-glycol mix in the loop have been well established through testing. The rate at which thermal energy is being transferred to or from the lab via the system can be calculated using the relationship:

$$\dot{Q}_{cooling} = C_p \cdot m \cdot (T_{out} - T_{in}) \quad [1]$$

where C_p is the specific heat of the glycol-water mixture, m is the mass flow rate of fluid in the chiller loop, and T_{out} and T_{in} are the leaving and entering temperatures of the gycol-water mixture at the cooling coil. The specific heat of the glycol is calculated by applying the linear correlation

$$C_p = 0.0025 \cdot T_{avg} + 3.7183 \quad [2]$$

where T_{avg} is the approximate average temperature of the fluid

$$T_{avg} = (T_{out} + T_{in}) / 2 \quad [3]$$

The mass flow rate of the fluid in the loop is calculated as

$$m = \rho \dot{V} \quad [4]$$

and the temperature-dependent density of the fluid is determined by

$$\rho = -0.0024x^2 - 0.2568 \cdot T_{avg} + 1040.2 \quad [5]$$

Equipment and Instrumentation

Surface temperatures were measured with Omega 44033 thermistors accurate to ±0.1 °C. The chiller loop temperatures were measured with one sensor on the downstream side of the condenser coil, while another sensor and an additional back-up sensor measured temperatures on the entering side of the condenser. The temperature of each of the interior surfaces in the lab was taken to be the average of at least four

readings. When exterior or interior blinds were employed, five dedicated thermistors were attached to the blind surfaces and the temperatures were averaged to give one temperature, which was assumed to be the isothermal temperature of all blinds. One temperature sensor per insulated exterior wall was employed, and at least four sensors were used to measure the external surface temperature of the façade. All thermistors attached to the façade were covered in a thin jacket of metallic tape to reduce their absorption of solar radiation and isolate the contribution of thermal flux from the façade surface. The temperature of supply air, return air, and center-of-room air were also measured. The definition of characteristic surfaces in the lab and the general arrangement of sensors are shown in the following figure.

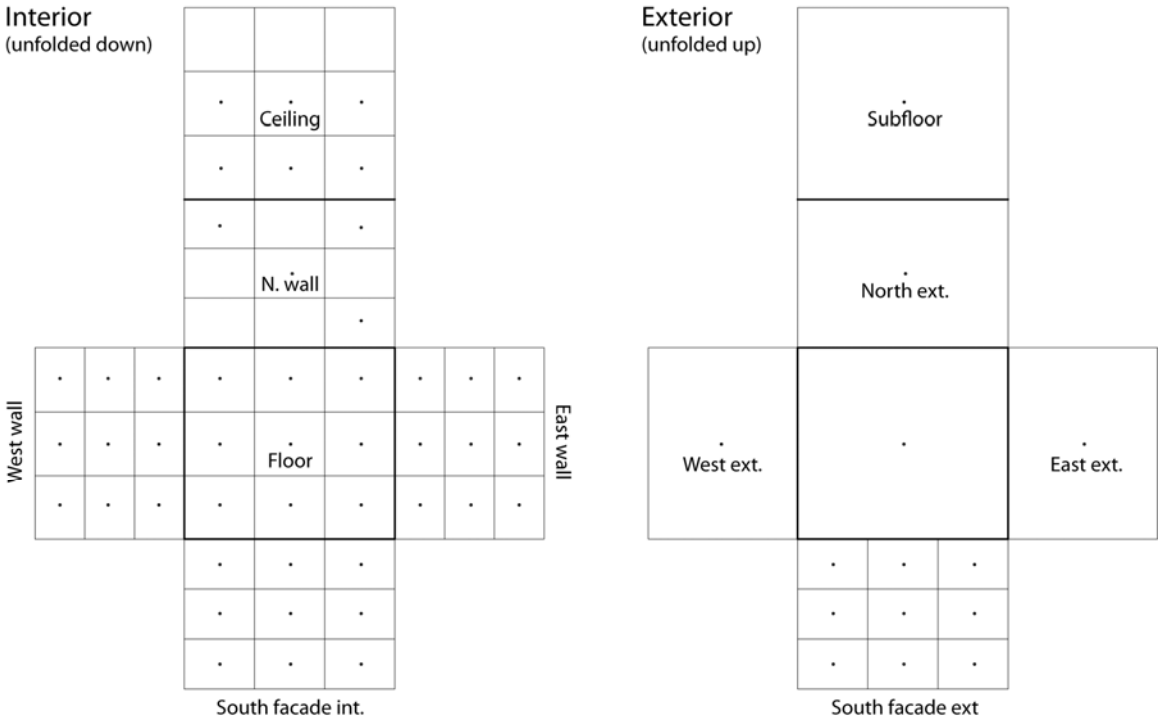

Figure 4.3: Thermistor arrangement on characteristic surfaces

The volumetric flow rate of fluid in the chiller loop was monitored with a field-calibrated flow meter with a known linear relationship ($R^2 = 0.9995$) between the output signal of the meter (pulses/sec) and the flow rate.

Electrical power of the room's equipment was measured with a Brand Electronic ONE power meter, accurate to ±1% of the measured value. The room equipment includes a blower motor, a PC and monitor, lights (left off for experiments), a power supply for the data loggers, a flow meter, and the power meter itself. The assumption is made that all power from the room equipment (a near constant 343 W) becomes a sensible thermal load within the test chamber. Integrating power consumption over time allows for the thermal loads due to environmental factors (solar radiation, and heat flux through the façade) to be isolated from the total cooling load.

Environmental conditions outside the lab were measured with a Davis Vantage Pro Plus weather station, with a temperature measurement accuracy of ±0.5°C at -45, -26, -18, 4, 27 and 60°C. The station measures global horizontal solar radiation with a silicon photodiode type pyranometer with a known cosine response and an accuracy of ±5% with up to ±2% drift per year. This pyranometer was field-calibrated using an Eppley Precision Spectral Pyranometer (PSP), which reproduces the WWR to within ±1%. A strong linear relationship was found between the two instruments using three days of readings ($R^2 = 0.973$) and this function was used to correct the Davis pyranometer readings. The weather station is also equipped with an anemometer, rain gauge, and humidistat.

The aforementioned Eppley PSP was fitted with a shadow band and used to measure global diffuse solar radiation. In addition, an Onset silicon pyranometer (S-LIB-M003) was installed near the plane of the lab's south façade to serve both as a backup for

the global horizontal radiation measurement, and to detect any shading that the façade might experience but which would not be measured by the other instruments. This sensor is accurate within ±10 W/m^2 or ±5%, whichever is greater. The same type of sensor was also installed on a stand inside the lab near the windows to measure transmitted solar radiation.

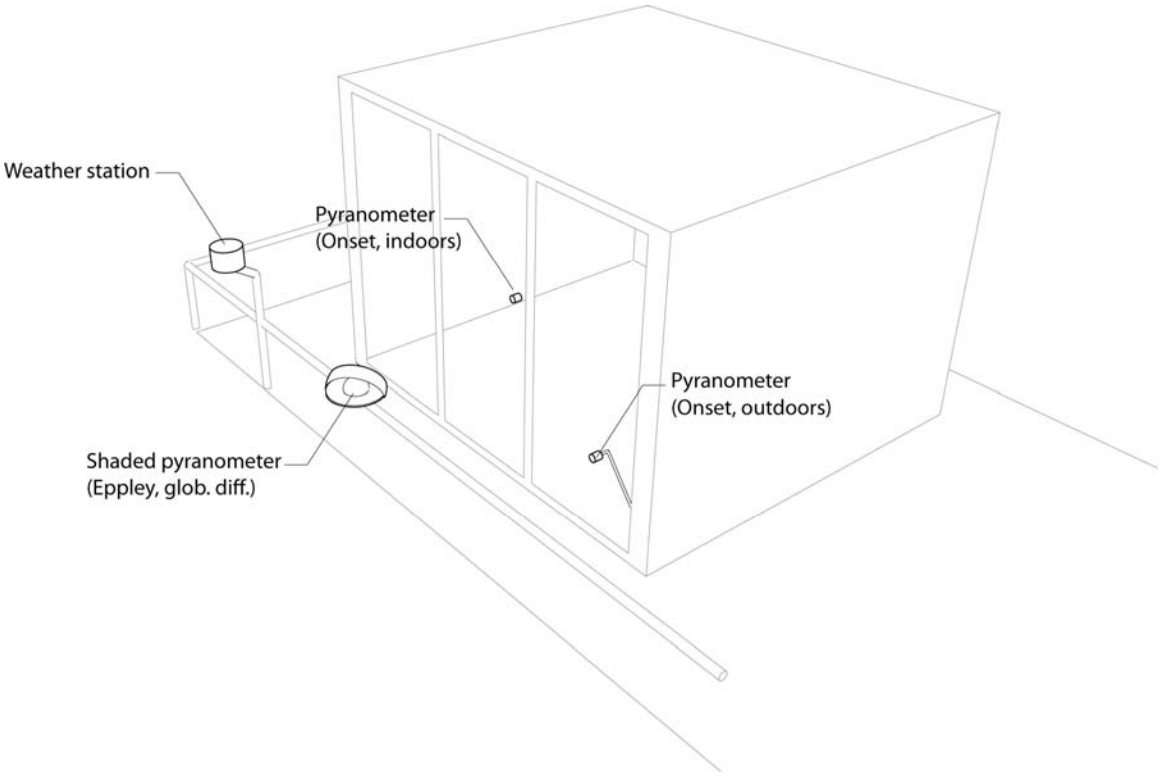

Figure 4.4: Arrangement of solar instrumentation and weather station

QUALITY CONTROL AND UNCERTAINTY ANALYSIS

A set of control measures was introduced to minimize the systematic or specific errors in the correlation development procedure. The following subsections briefly describe these control measures.

Pre-experiment test runs for measurements and sensor monitoring

In the first phase of the project, a group of experiments was repeated to identify faulty sensors. A significant number of thermistors were replaced, and follow-up monitoring was conducted to confirm their performance. A persistent intermittent fault in the logging of cooling coil temperatures—a key measurement for the experiments—was detected and eliminated before recording data for the final experimental runs. All final experiments were run for approximately 24 hours, with data recorded at one-minute intervals. The raw data was analyzed for obvious errors in logging and/or processing before proceeding to the next experiment.

Minimizing relative error in key metric

A relatively low mass flow rate was specified for the cooling system. The effect of this is increase the magnitude of the temperature change across the cooling coil, thus reducing the relative measurement error in the calculation of the temperature difference.

Maintenance of consistent testing chamber conditions

The lab was kept sealed for most of each 24-hour testing period so as not to introduce unmeasured loads to the chamber. The lab was entered at the same time on each experiment day—roughly 1 hour before sunrise—to adjust blind settings, and time spent inside for these processes was logged and minimized. The door to the lab was sealed after entering and leaving. A humidity logger was placed in the return air plenum

of the lab to enable monitoring of dew point temperature in the lab. No significant change in indoor absolute humidity levels was detected during the experiments.

Development of a data processing template

To reduce the steps involved in data processing for each experiment, and thus reduce the chance of introducing systematic error, a data processing template was configured in Excel. This allowed for simple importing of the raw data tables from the various logging systems in the lab. The template was tested over several days during calibration of the lab and before experiments began. The template was partially reviewed by a doctoral student who monitors the lab, to check for errors in the calculation of the primary metric, $\dot{Q}_{cooling}$.

Uncertainty

Assuming a near perfect air-tightness in the lab, the primary metric—cooling power—captures thermal flux from equipment and through the south façade. Cooling power can be quantified as:

$$\dot{Q}_{cooling} = C_p \cdot m \cdot (T_{out} - T_{in})$$

Uncertainty is given as a function of the imprecision inherent in all variables used to calculate a reported value. As the key results of the current investigation are based the rate of thermal energy being removed from the lab the following uncertainties are applicable:

Variable	Instrument Used	Accuracy
Coil Temperature (in)	Omega 44033 thermistors	±0.1 °C
Coil Temperature (out)	Omega 44033 thermistors	±0.1 °C
Coil flow rate	Omega FTG-9500	2% of measured value
Specific heat of fluid	Experimentally tested	Assumed exact
Density of fluid	Experimentally tested	Assumed exact
Surface temperatures (blind slats, windows, room surfaces)	Omega 44033 thermistors	±0.1 °C
Internal equipment loads	Brand Electronic ONE power meter	±1%
Global horiz. Radiation 1	Davis 7821	Data post-processed using correlation with Eppley PSP (R^2=0.973)
Global horiz. Radiation 2	Onset pyranometer S-LIB-M003	Greater of ±10 W/m^2 or ±5%
Global diff. radiation	Eppley PSP	Within ±1% of WRR
Global normal radiation (interior)	Onset pyranometer S-LIB-M003	Greater of ±10 W/m^2or ±5%
Outdoor air temp	Davis External temp sensor	±0.5°C under 43°C
Wind direction	Davis Anemometer 6410	±4 degrees
Wind speed	Davis Anemometer 6410	Greater of ±3 km/h or ±5%
Precipitation	Davis Rain collector II	Calibrated 0.01" (0.003 m) increments

Table 4.3: Uncertainties in experimental measurements

With error due to each measurement determined, the effect on the final value calculated is then determined. For the purposes of the current investigation, the general uncertainty theory given in ASHRAE (2000) is employed in the calculation of the error in the final values reported: $\dot{Q}_{cooling}$.

$$\delta\phi = \sqrt{\sum_i^n \left(\delta u_i \frac{d\phi}{du_i}\right)^2} \qquad [6]$$

where $\delta\phi$ is the uncertainty in the considered value,

n is the number of parameters used in the equation for calculation of considered value,

δu_i is the uncertainty in the particular parameter and

$\frac{d\phi}{du_i}$ is the change in the considered value with a unit change of the parameter in question.

As the cooling rate is derived from the mass flow rate of fluid in the cooling coil ($\dot{m}$) and reference temperature difference (ΔT: fluid leaving – fluid entering) the uncertainty in the convection coefficient is calculated based on:

$$\delta \mathrm{Q} = \sqrt{\left(\delta \dot{\mathrm{m}}\right)^2 + \left(\frac{\delta\ \Delta T}{\Delta T}\right)^2} \qquad [7]$$

The uncertainty in temperature difference is calculated by uncertainty in leaving (δT_{out}) and entering (δT_{in}) fluid temperature:

$$\delta\,\Delta T = \sqrt{\left(\delta\, T_{out}\right)^2 + \left(\delta\, T_{in}\right)^2} \qquad [8]$$

EXPERIMENTAL MATRIX

Six experiments were run with different shading configurations on the south façade of the lab. For experiments using fixed-angle slat-type blinds, blind angle was adjusted and carefully confirmed with a protractor. Blind configuration was the only aspect changed from experiment to experiment. For external blinds, the distance from glass to blind edge was 0.15 m; the gap between internal blinds and the window was 0.09 m.

Cooling set point, fan flow rate, and internal equipment gains were identical for all scenarios. Air exiting the fan coil unit (FCU) was delivered to two slot diffusers located just inside the south façade, at a rate equivalent to approximately 12 air-changes per hour (ACH). One hundred percent return air re-entered the FCU through a return plenum on the north wall. The position and type of the diffusers and the velocity of the supply air needed to be considered when developing a simulation model of the lab flowing the experimental phase, as this affects temperatures, flow regime, and thus convection rate at the facade/internal blind layer. This is discussed further in the section of this chapter that describes the modeling methodology.

Position	Slat angle	Slat width/spacing	Slat material	Slat τ	Slat ρ	Slat ε
None	n/a	n/a	n/a	n/a	n/a	n/a
External	45°	8 cm / 5.25 cm	Metallic painted aluminum	0	0.8	0.9
Internal	90° (flat)	2.5 cm / 1.88 cm	Black vinyl	0	0.2	0.9
Internal	45°	2.5 cm / 1.88 cm	Black vinyl	0	0.2	0.9
Internal	90° (flat)	2.5 cm / 1.88 cm	White painted aluminum	0	0.8	0.9
Internal	45°	2.5 cm / 1.88 cm	White painted aluminum	0	0.8	0.9

Table 4.4: Experimental Matrix. Slat ρ = beam and diffuse solar reflectance. Slat ε = longwave hemispherical emissivity.

SIMULATION METHODOLOGY

Using known properties of the lab assembly and systems, a simulation model was developed using the EnergyPlus whole building simulation program.

The comparisons made for purposes of the validation use cooling energy as the sole metric. Cooling power was required at all times in the lab due to the baseline of internal equipment loads. This measure neatly captures all the information necessary to judge the performance of the software algorithms. A finer grained examination of experimental data and simulation outputs can also be used to examine specific components of the algorithm—for example, the criteria for dynamic selection of convection coefficients on surfaces, or the amount of solar radiation entering the space through the blinds.

The validated models can then be used in lieu of parallel experiments in order to estimate cooling energy for other blind or shading configurations. The model inputs can also be used to test other scenarios, such as different site orientations and configurations of multiple offices to estimate the effect on cooling energy of the various shading strategies.

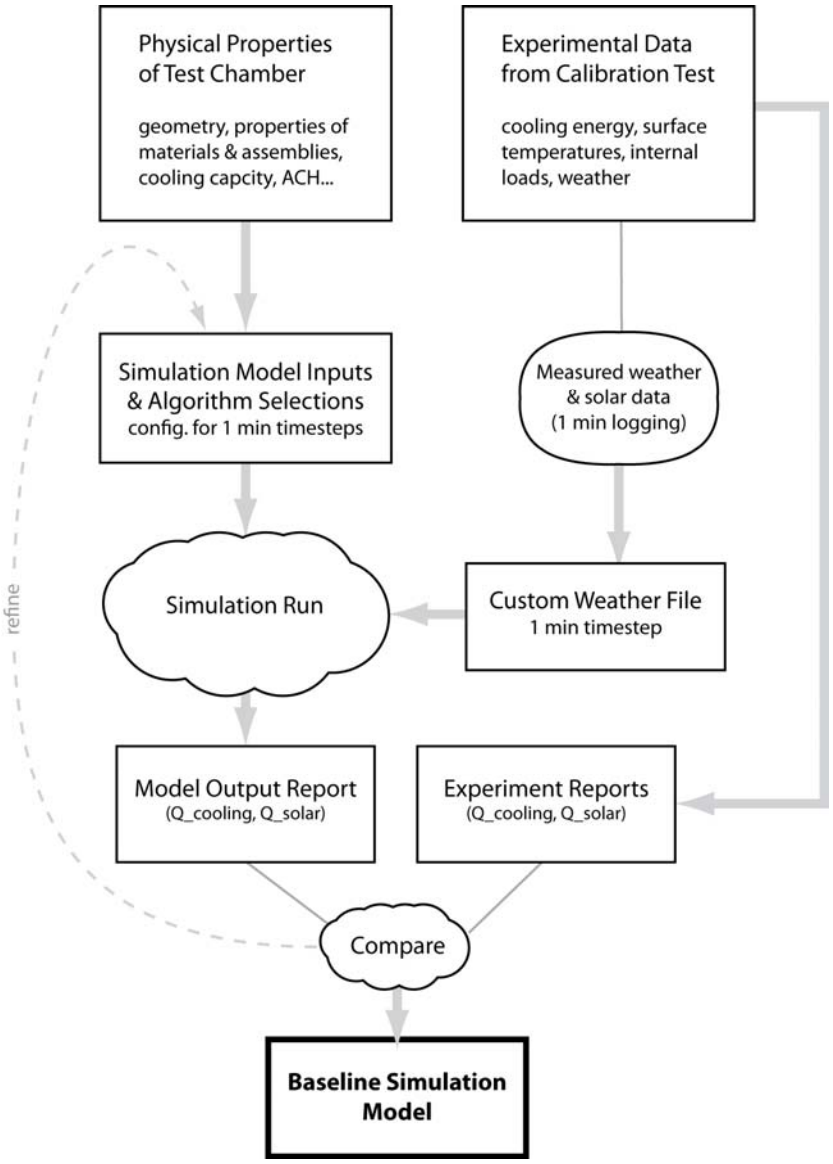

Figure 4.5: Process for development of the baseline simulation model

Development of the Model

A simulation model of the testing facility was constructed in EnergyPlus. Whenever possible, material properties of assemblies and components were modeled using values derived during calibration testing of the lab performed in 2009. When such

values were not available, properties were taken from the ASHRAE Handbook of Fundamentals (HoF). The dimensions of the lab shell have been precisely measured, and the resulting data were used as the basis for the model geometry. The following sections give more detail about the creation of the model.

Properties of Wall Assemblies

The walls of the lab chamber were designed to simulate an approximately adiabatic wall condition that would be found between spaces in office buildings with identical conditions, such as neighboring offices. Thermal flux through these surfaces (the floor, ceiling, and walls other than the façade) is assumed to have negligible effect on the conditions inside the lab. The walls were modeled using as-built layers of the lab, and using material properties form the ASHRAE HoF. This resulted in walls with an average U-value of 0.085 W/m^2K, which is slightly lower than a value for one of the walls measured in 2009 of 0.099 W/m^2K. The difference is assumed to have no effect on modeling results.

Properties of the South Facade

The south façade represents the origin of the entire environmental thermal load in the sealed lab. This façade has not been separately tested to determine an overall U-value, so there is some uncertainty about the rate of conduction through the frame and at the frame/window interface. EnergyPlus contains a module that allows for detailed modeling of window frames in order to account for heat transfer through the frame elements as well as edge effects at the window/frame junction. Precise properties for the frame were not available, so values for a typical thermally-broken aluminum frame were imported from the IGDB frame database. Overall properties of the windows themselves, listed near the beginning of this chapter, are well-known, and were taken from LBNL's International

Glazing Database (IGDB) and checked against manufacturer cut sheets. WINDOW6 window simulation software was used to calculate average properties of the window glass and a ratio of frame edge to center of glazing conductance.

Solar flux is a key variable in these experiments, so the south façade of the lab was precisely measured to accurately account for shading due the aluminum frames of the curtain wall and an overhanging external blind storage compartment. This box can create significant shading at high solar angles that occur during Austin's summer months.

Properties of the Cooling System

The cooling system was modeled in EnergyPlus as an "ideal loads" system. This system type allows for direct reporting of the amount of thermal energy removed from the simulated lab without having to back out values from system component efficiencies. The cooling capacity limits for the modeled system were set at the manufacturer's reported value of 5275 W and air flow rate through the fan coil corresponds to approximately 12 air changes per hour (ACH) as measured at the diffusers. The system maintains the simulated room air at a set point of 21.4 °C with no deadband.

Internal loads

Internal loads due to equipment were found to be a near constant 344 W. This average value was used in the simulation model, and acts essentially as a 100% convective (instantaneous) load.

Selection of algorithms

Three algorithms were specified for calculating heat transfer in the model: a heat balance algorithm, which calculates temperatures at surface, internal, and air nodes for each timestep of the simulation; an internal convection algorithm, which dynamically calculates a convection coefficient for each surface of the room at each timestep; and an

external surface convection algorithm. One minute timesteps were used for the simulation.

Heat balance

For heat balance, a semi-implicit conduction finite difference method was employed. This algorithm was selected for its ability to model transient conduction, in order to capture heat storage in the mass of the double-layer gypsum walls and two-layer plywood floor of the lab. EnergyPlus uses the following four types of nodes, as shown in the figure below (1) interior surface nodes, (2) interior nodes, (3) material interface nodes and (4) external surface nodes. The grid for each material is established by specifying a half node for each edge of a material and equal size nodes for the rest of the material. Surface discretization also depends on the thermal diffusivity of the material (α) and time step (ΔT) selected.

Internal convection

The internal convection algorithm uses several properties of the model to calculate the convection coefficient at each timestep. It is based on classifying surfaces by flow regime and orientation so that the correct equation can be chosen at a particular point in time during the simulation. The classification depends on user input with some aspects processed only once at the beginning and others during each timestep. There are also various parameters or inputs to the convection equations that need static or dynamic processing. Each surface in the model is examined to determine its type (floor, wall, ceiling), tilt angle, and characteristic height. The user input for air flow rate of the HVAC system is used for forced or mixed convection correlations. During the simulation, each surface is evaluated to determine convection stability as a function of ΔT. The algorithm

switches between forced, mixed, and natural flow regimes by calculating the Richardson number, Ri = Gr/Re^2, for the zone. Large values of Ri indicate buoyancy dominates, while small values indicate forced flows dominate. EnergyPlus assumes that central air type equipment with diffusers forces air down walls.

These inputs were processed using a user-specified set of convection coefficient correlations. The Thermal Lab, as configured for the experiments described in this paper, is essentially a representation of a highly glazed perimeter zone served by slot diffusers. Therefore, a set of appropriate correlations was used for the model. The façade wall and the floor were modeled using equations developed by Goldstein and Novoselac (2010) for forced air situations with ceiling slot diffusers along perimeters with significant glazing fractions.[3] For a wall with glazing fraction > 50% :

$$h=0.103\ (\dot{V}/L)^{0.8} \qquad [9]$$

For the floor:

$$h=0.048\ (\dot{V}/L)^{0.8} \qquad [10]$$

where $\dot{V}$ is the volumetric flow rate of air from the diffusers, and L is the characteristic length of the surface.

Convection on the ceiling was modeled using an equation developed in 1997 by Fisher and Pedersen based on laboratory chamber measurements.[4] The convection coefficient is calculated as:

$$h = 1.208 + 1.012 * ACH^{0.604} \qquad [11]$$

[3] Goldstein, K. and Novoselac, A. (2010)
[4] Fisher, D. E., and C. O. Pedersen. 1997.

For the other walls, an adaptive algorithm was selected, which dynamically chooses a convection model at each timestep based on calculated conditions at the surface.

External convection

External convection was modeled using the "DOE-2" convection coefficients. For smooth surfaces (the window glass), the coefficient is based on measurements taken at the Mobile Window Thermal Test (MoWiTT) facility by Yazdanian and Klems in 1994. It is calculated as:

$$h_{c,glass} = \sqrt{h_n^2 + [aV_z^b]^2} \qquad [12]$$

where h_n is the natural convective heat transfer coefficient formulated by Walton (1983) and depends on surface orientation and the temperature difference between the surface node and T^{∞}, and a and b are constants selected based on wind speed and direction relative to the surface.

For slightly rough surfaces:

$$h_c = h_n + R_f (h_{c,glass} - h_n) \qquad [13]$$

where R_f is a roughness multiplier derived from user inputs of surface layer material properties. Complete documentation of the convection algorithms is available in the *EnergyPlus Engineering Reference*.[5]

Weather data

A custom weather file in the EPW format was created for each simulation using data collected on the day of the physical experiment by the instruments described earlier in this chapter.

Other considerations

For each simulation, the model was run through a 20-day warm-up period in order to "charge" internal surfaces with heat storage capacity. This was done to mimic conditions in the actual lab, which has been continuously exposed to outdoor weather in the summer months prior to the beginning of the experiments.

[5] EnergyPlus Development Team. 2010.

Chapter 5: Results and Discussion

This chapter presents the results of the experiments and corresponding models. It also provides a critical analysis of the results, including a description of difficulties and challenges in various aspects of the study.

Each experiment was conducted over 24 hours in an outdoor test chamber under real weather conditions. Since the individual experiments were conducted on different days, with different solar and weather conditions, cooling loads cannot be directly compared to assess the relative performance of the blinds. The comparison of experiments is made by quantitatively comparing cooling energy with a qualitative analysis of weather conditions for the different experiment days. Experimental cooling data is presented as profile of average hourly cooling power for the duration of the experiment, alongside a sum of the thermal energy removed from the lab (cooling energy) during the experiment. Simulation model performance is also shown for comparison. Total daily global horizontal solar radiation, temperature data (high, low, average), and wind run are supplied as outdoor weather parameters that have the greatest likely effect on cooling energy in the chamber.

WEATHER COMPARISON

Global horizontal radiation data for each experiment day is totaled for one square meter of surface area and presented to represent the relative intensity of solar energy for each experiment. Since experiments were conducted over an 11 day period spanning from July 23 to August 3, incident beam solar angles on the vertical surface of the lab are very similar, and effects of their difference can be reasonably ignored. No experiment day was heavily cloudy, so timing of peak solar was identical for all days.

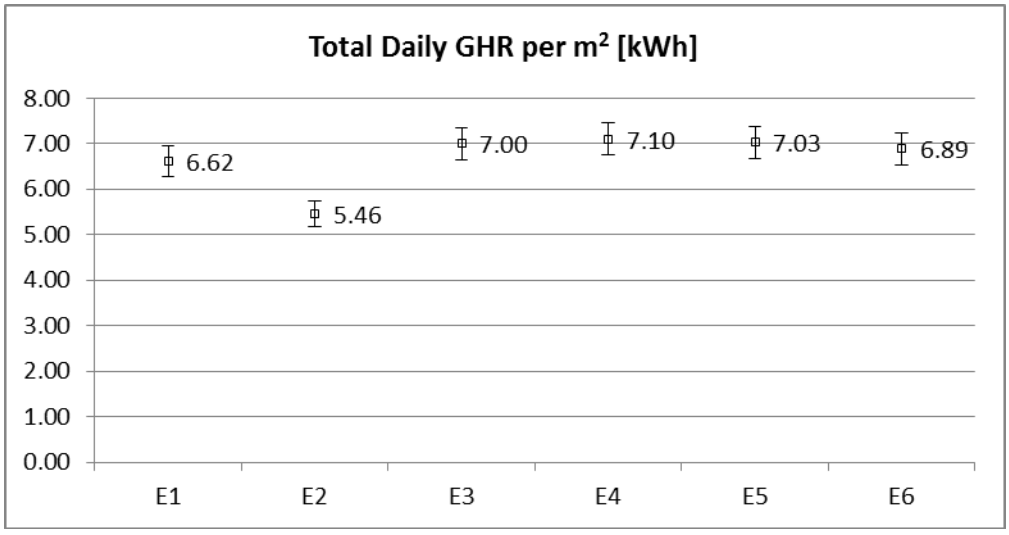

Figure 5.1: Daily total global horizontal radiation (GHR) for experiment days

During the testing period, peak outdoor temperature occurred, on average, at 16:41 local time (CST) with earliest peak temperature at 16:38 and latest at 16:42. The average, maximum, and minimum temperatures are presented for comparison.

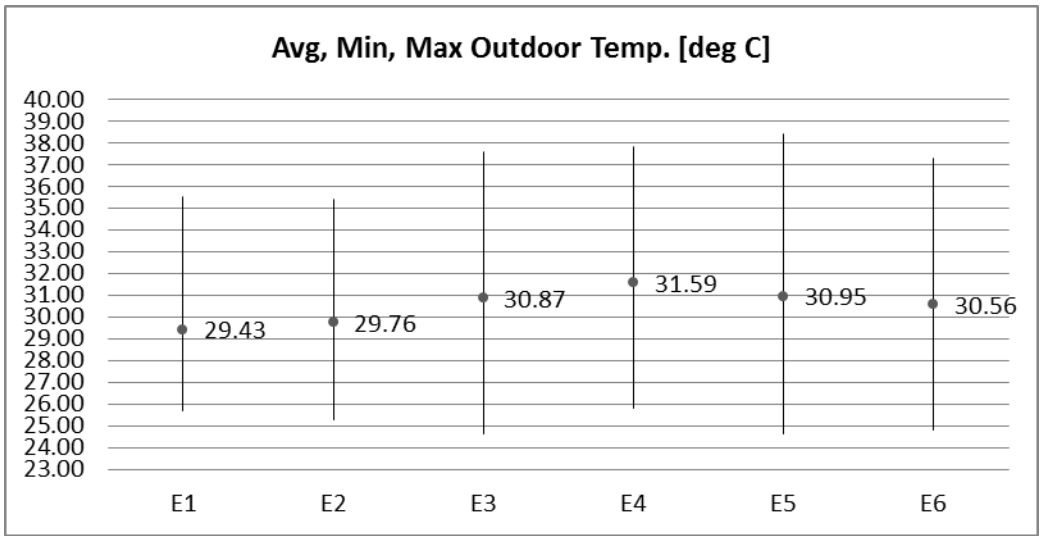

Figure 5.2: Outdoor air temperature data for the experiment days. Average temperature labeled; bars indicate the range of daily temperature.

Outdoor wind can influence convection rates on the test chamber's exterior surfaces. The final weather metric, "wind run" is a means to capture the relative windiness of the testing days. It is calculated automatically by the weather station by multiplying wind speed [m/s] and the duration of the wind event [s]. The daily wind run does not capture when the individual wind events occurred, and is not a good measure of average wind speed; therefore, the full wind record is also included for reference.

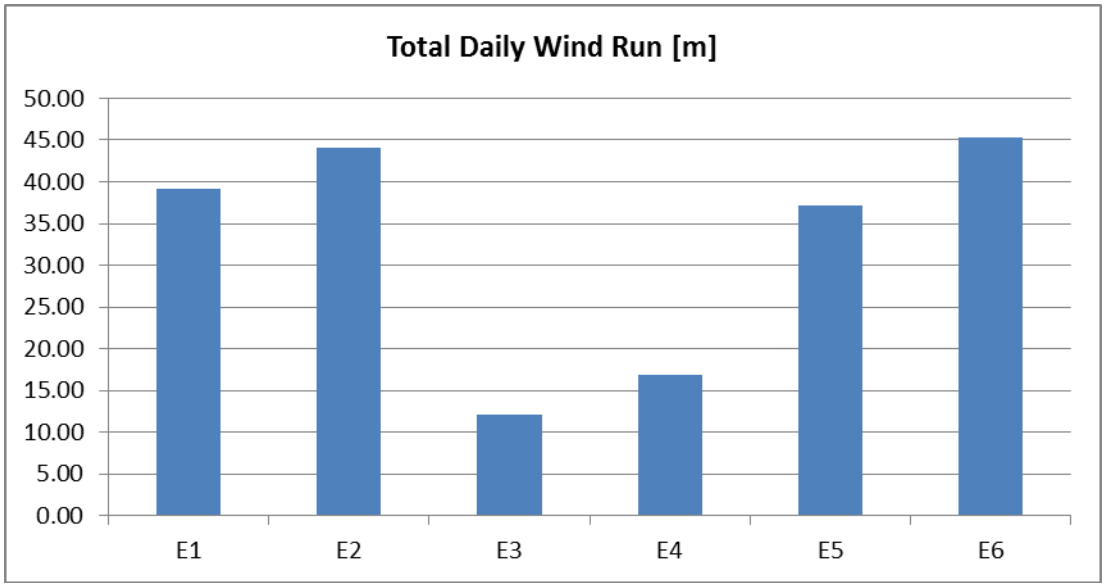

Figure 5.3: Daily wind run for experiment days

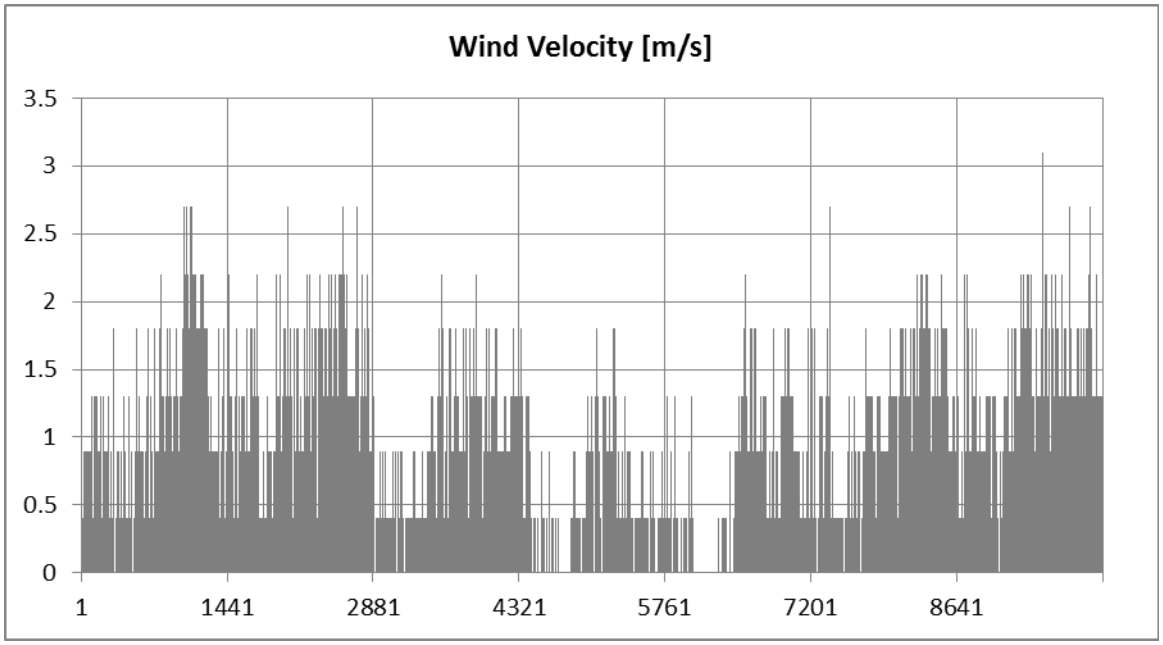

Figure 5.4: Instantaneous wind velocity for experiment days. Averaged 1 min intervals. Vertical lines separate experiment days. E1-E6 appear in order from L to R.

MEASURED COOLING ENERGY AND SIMULATION RESULTS

Calibration Experiment

The test chamber was configured with no blinds in order to test the agreement between the experiment and model for exterior normal incident solar radiation and solar flux through the façade layer. This also established a baseline against which to measure the performance of the simulation model before adding the various blind models.

Verification of incident normal solar radiation

The first table shows the two components of solar radiation measured on the test day—diffuse horizontal radiation and global horizontal radiation—and the calculated direct horizontal component resulting from their difference.

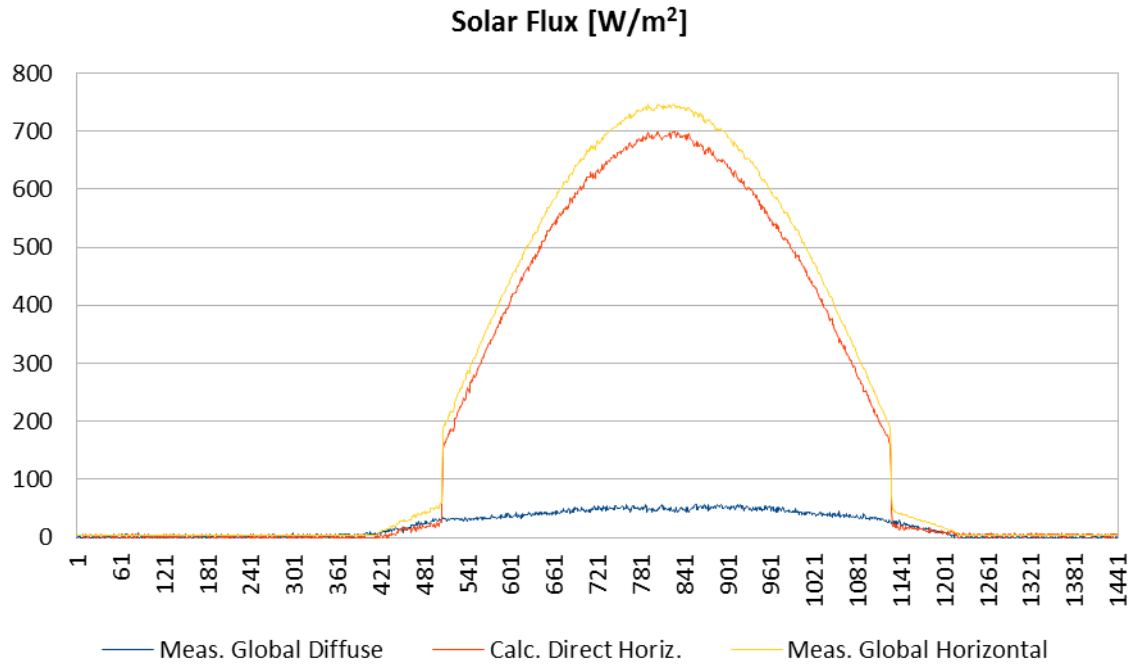

Figure 5.5: Calculation of direct horizontal solar radiation from measured components on test day (Aug. 3).

The direct horizontal radiation component and global horizontal radiation components are included in the weather data for the simulation. From the direct horizontal component, the simulation algorithm calculates direct incident radiation using solar angle and surface angle corrections, and then calculates total incident normal radiation for each surface resulting from global diffuse and direct normal components. Normal incident radiation was measured at the test facility for the calibration day and compared to the model estimation. The experimentally measured incident radiation for an un-shaded vertical surface under these conditions shows good agreement with the values calculated by the model from the component inputs. Results are shown Figure 5.6.

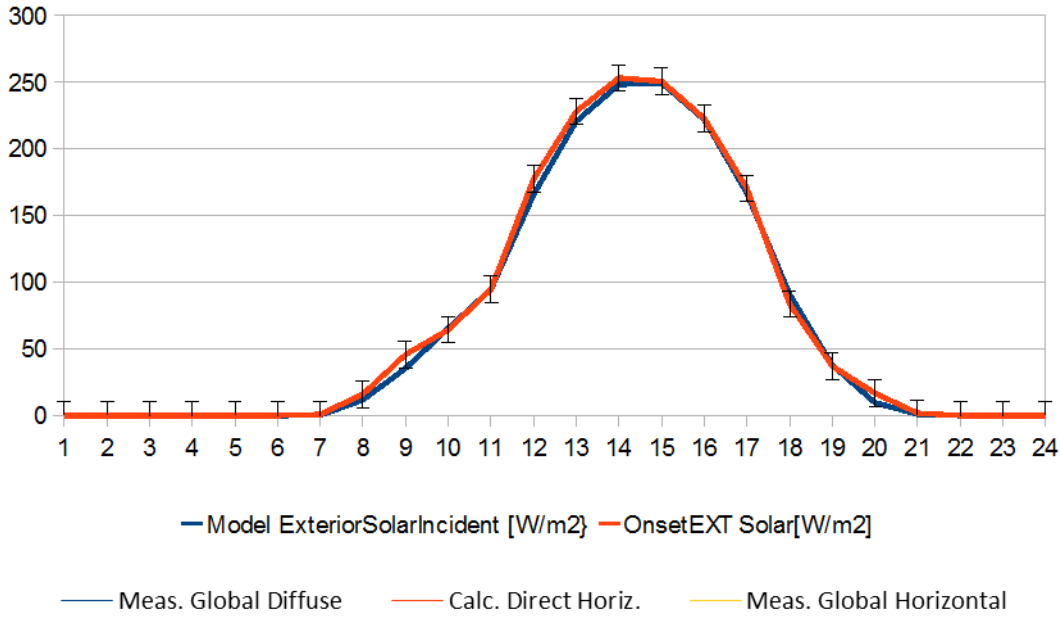

Figure 5.6: Comparison of measured and modeled incident solar on the thermal lab façade for the calibration day (Aug. 3).

Finally, the measured and modeled transmitted solar flux was compared. Modeled transmitted solar was observed to fit within the known error range of the sensor.

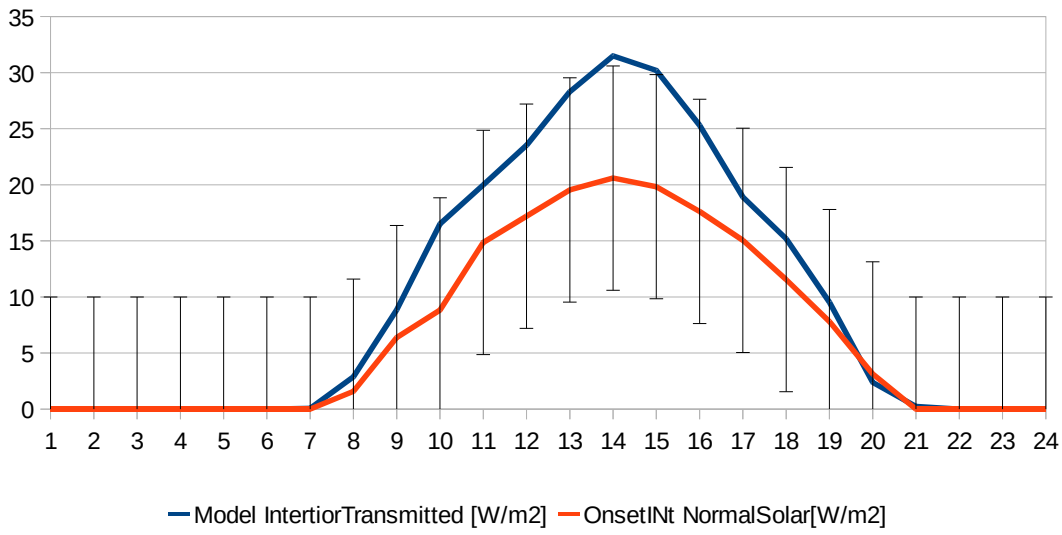

Figure 5.7: Comparison of transmitted normal solar flux to the inside of the thermal lab.

Experiment 6 (E6): No blinds

The hourly cooling graph shows average cooling power for each hour of the experiment. The overlay of modeled cooling power shows good agreement with the experiment both in terms of magnitude of cooling power and timing of peak cooling energy. The measured and modeled internal equipment power are also shown. This is assumed to represent all sensible gains from internal sources in the test chamber, and subtracting this from the cooling energy gives a measure of gains from the outdoor environment through the façade.

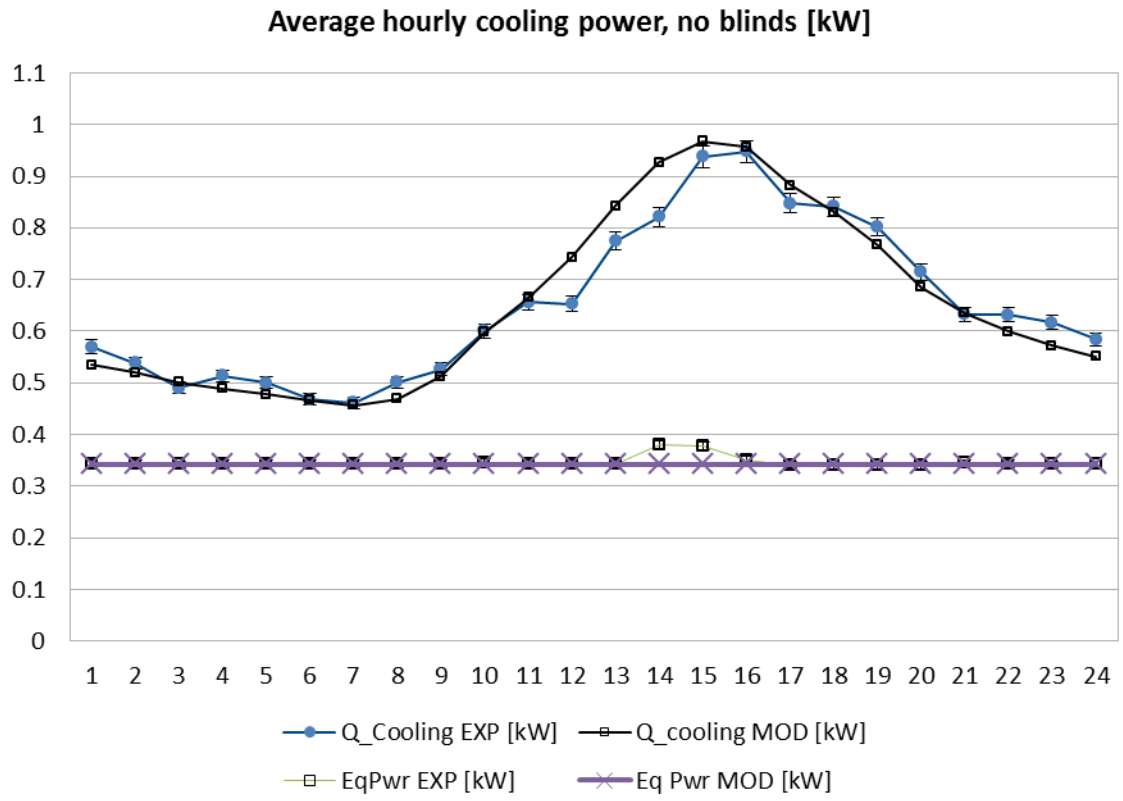

Figure 5.8: Average hourly cooling rate, no blinds [kW].

Measured daily total cooling energy on the calibration day for the facade with no blinds was 15.63 kWh. The model showed good agreement for cooling energy, with a total of 15.65 kWh. Global horizontal radiation energy for this day was slightly above the average of all experiment days—6.89 kWh/m^2 versus 6.68 kWh/m^2. The average temperature was very close to the average for all experiments 30.56 ºC versus the overall average of 30.53 ºC

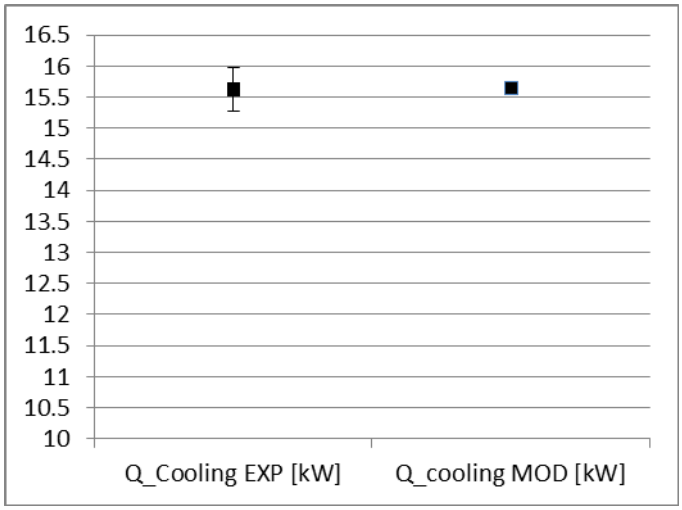

Figure 5.9: Measured and modeled total cooling energy for the experiment, no blinds.

It was judged that this model was in good agreement with the experimental results, and was used as the basis for all subsequent models.

Experiment 1 (E1): Exterior blind, slats at 45º

This case used an exterior aluminum blind with 0.08 m wide slats and 0.0525 m slat spacing, with the assembly mounted 0.15 m away from the outside of the facade. The blind slats were adjusted to 45-degrees. It was hypothesized that this experiment would yield the lowest relative removal of cooling energy from the lab, as the external blind prevents some portion of beam solar from ever reaching the test chamber's façade. An unexplained bump in cooling power occurs in the experiment in the fourth hour.

The measured daily total cooling energy was 12.68 kWh. The model predicted a total cooling energy of 12.11 kWh. The peak cooling energy in the model is slightly lower, and occurs earlier than in the experimental case.

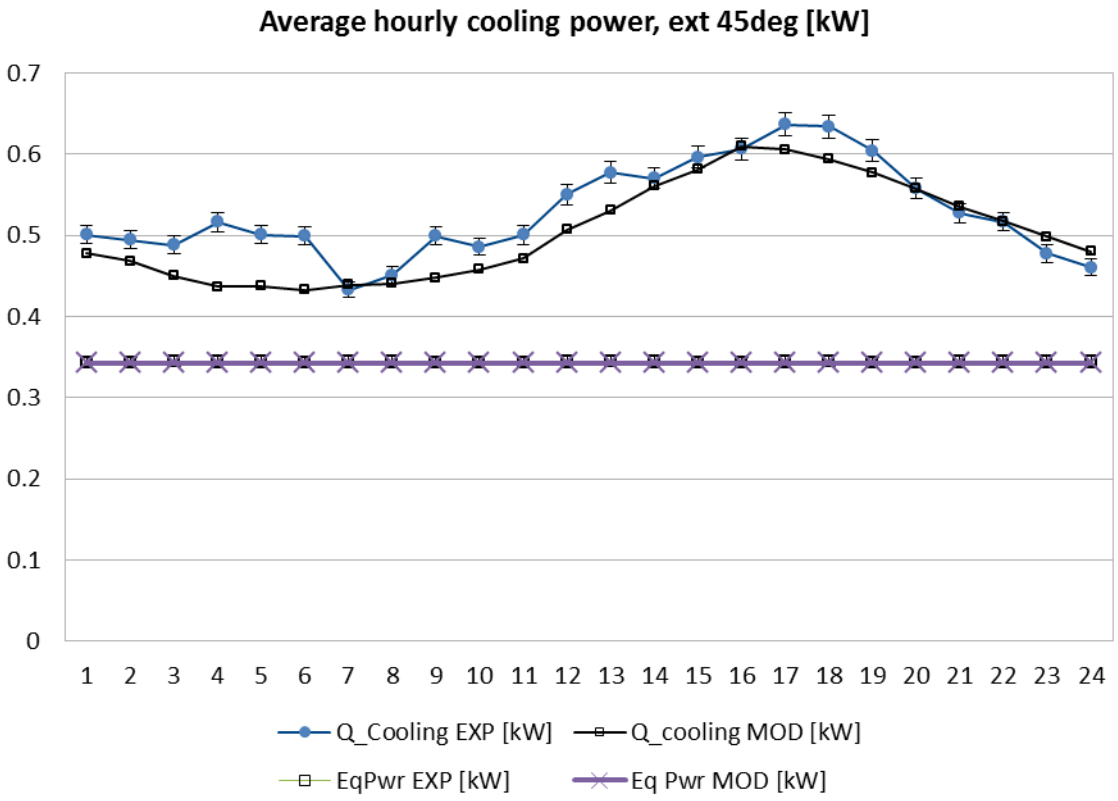

Figure 5.10: Measured and modeled total cooling rate, ext, 45º.

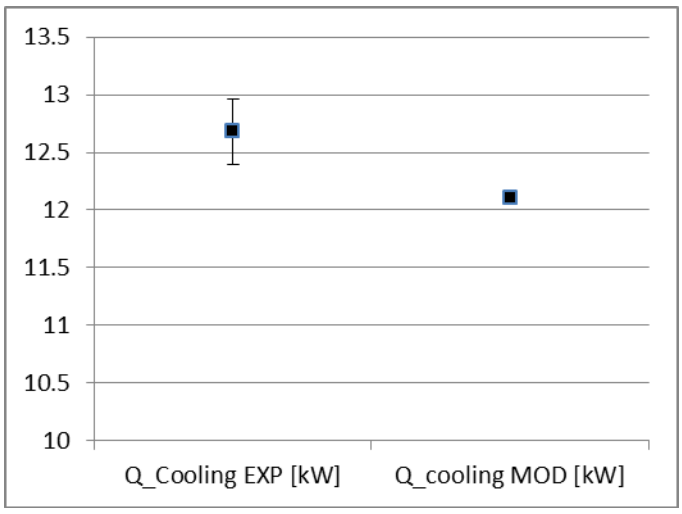

Figure 5.11: Measured and modeled total cooling energy for the experiment, ext 45º.

The total GHR for the day of this experiment was 6.62 kWh/m2, which is slightly below the average for all experiments. Average temperature was also slightly below the average, 29.43 ºC versus the overall average of 30.53 ºC.

Experiment 2 (E2): Interior blind, black, slats at 90º

The blind for this case has black vinyl slats with integral color, and 0.0254 m slat width. The blind was mounted at 0.92 m from the internal surface of the window with slats adjusted to 90º (flat). Part of the interest of this experience was to test previously published studies that reported that dark interior blinds can not only fail to reduce solar energy transmitted into a room (due to very low reflectivity), but can increase the instantaneous rate of convection, and increase peak cooling load.

The weather for this experiment showed the lowest GHR of any experiment (5.46 kWh/m^2) and a below average outdoor temperature (29.76 ºC). Measured daily total cooling energy was 14.24 kWh. The model predicted a total cooling energy of 13.99 kWh. There is also good agreement in magnitude and timing of peak cooling energy.

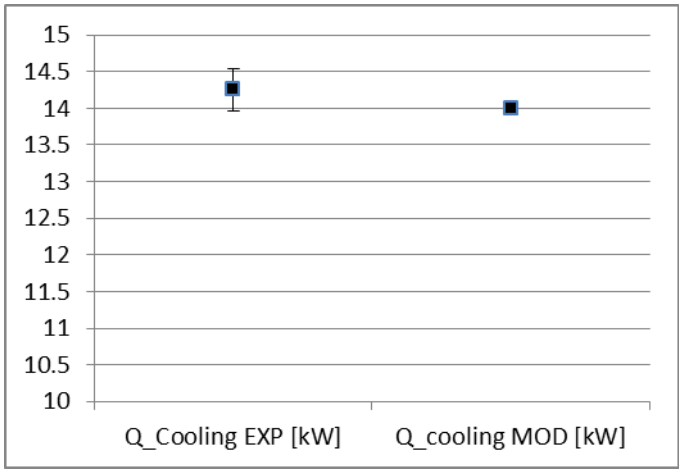

Figure 5.12: Measured and modeled total cooling energy, int. black 90º.

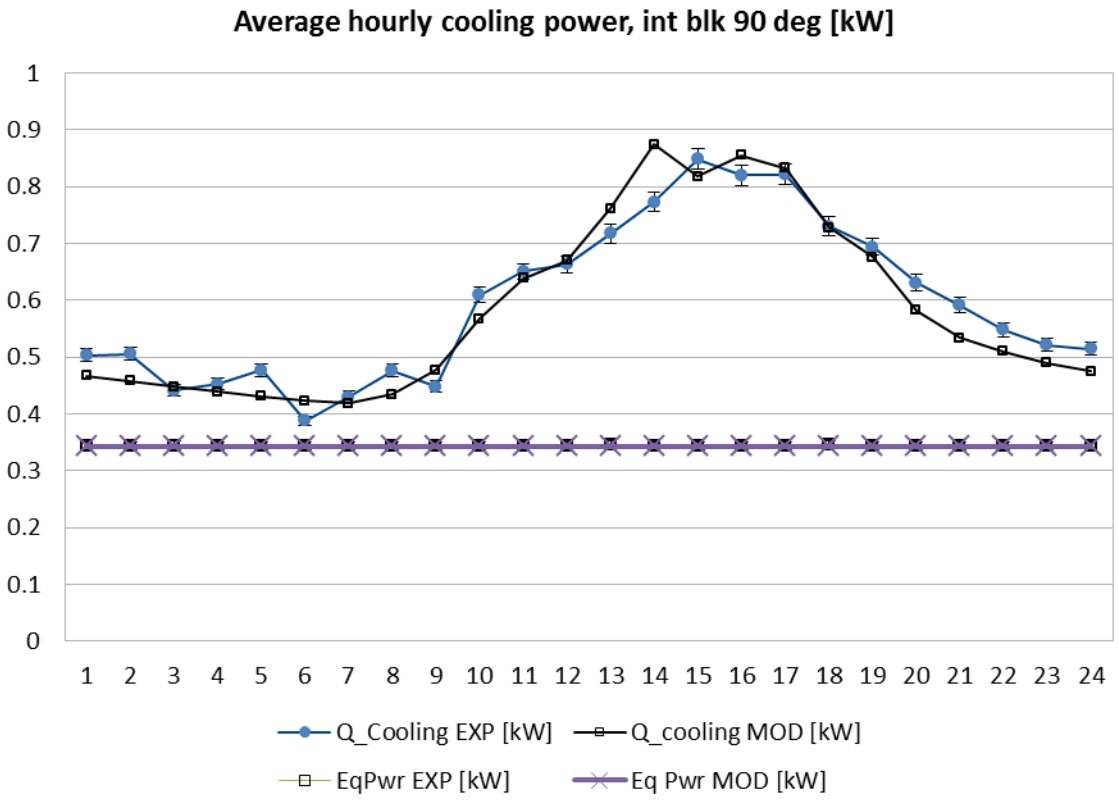

Figure 5.13: Measured and modeled cooling rate, interior black blind, 90º.

Experiment 3 (E3): Interior blind, black, slats at 45º

This experiment uses the same black blinds described for the 90-degree case, but with the slats adjusted to 45-degrees. Due to problem in data recording after 21h, the experimental results are terminated at 21h. The measured daily total cooling energy to that point was 13.25 kWh. The model predicted a total cooling energy of 12.29 kWh. The modeled peak energy is lower than for the observed case.

The measured GHR for this day was 7.0 kWh/m^2 and the average temperature was 30.87 ºC.

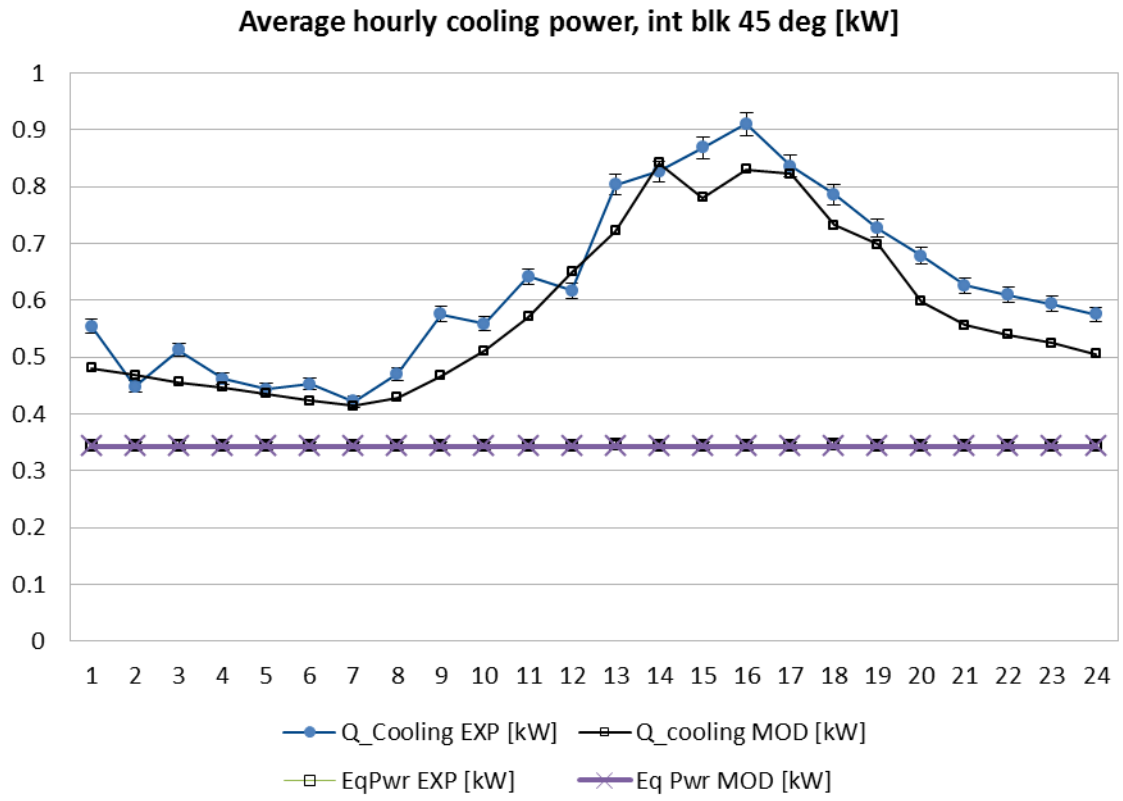

Figure 5.14: Measured and modeled cooling rate, interior black blind, 45º.

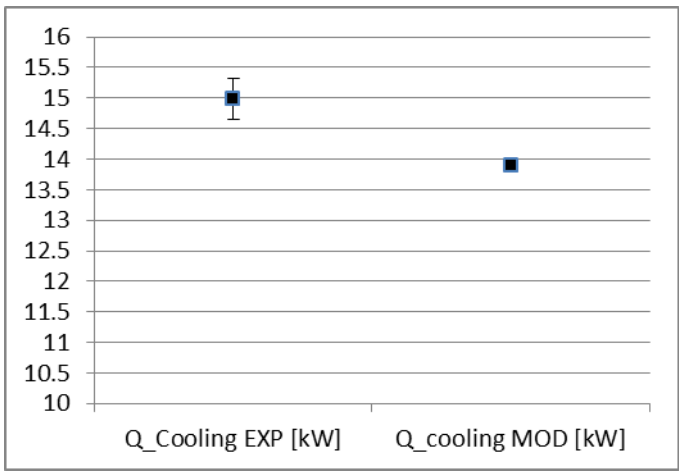

Figure 5.15: Measured and modeled total cooling energy, int black blind, 45º.

For the experimental case, cooling power can be interpolated for the three missing hours, following the trend of the modeled energy. This results in an experimental cooling energy of 15.00 kWh and the modeled cooling energy until 24h is 13.90 kWh. These values will be used in a comparative analysis of all the experiments.

Experiment 4 (E4): Interior blind, white, slats at 45º

This experiment uses aluminum blinds painted white, with slat geometry identical to the black vinyl blinds. The white blinds were expected to lower cooling energy compared to a no-blinds case, as their reflectivity causes them to reject some portion shortwave solar energy back out through façade.

Measured daily total cooling energy was 15.56 kWh. The model predicted a total cooling energy of 13.87 kWh. The modeled peak energy is lower than for the observed case.

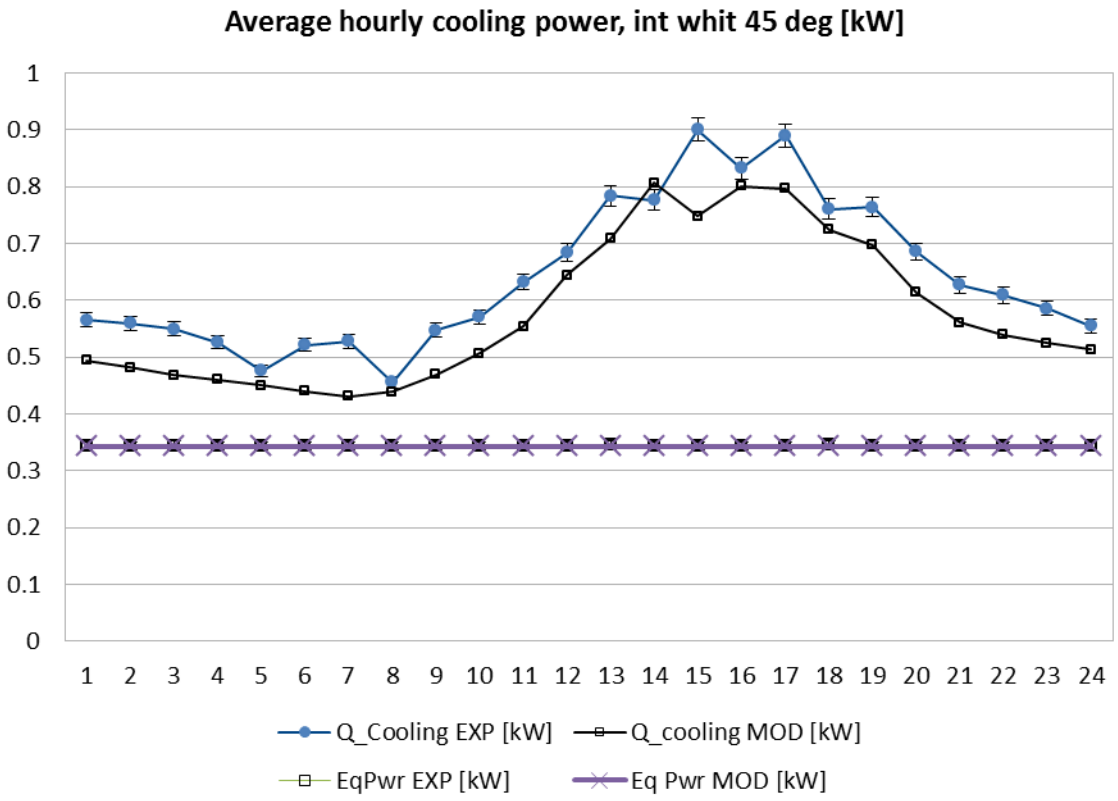

Figure 5.16: Measured and modeled cooling rate, interior white blind, 45º.

The GHR was higher on this day than for any other experiment (7.10 kWh/m^2) and the average temperature was just greater than 1 ºC above the average (31.59 ºC).

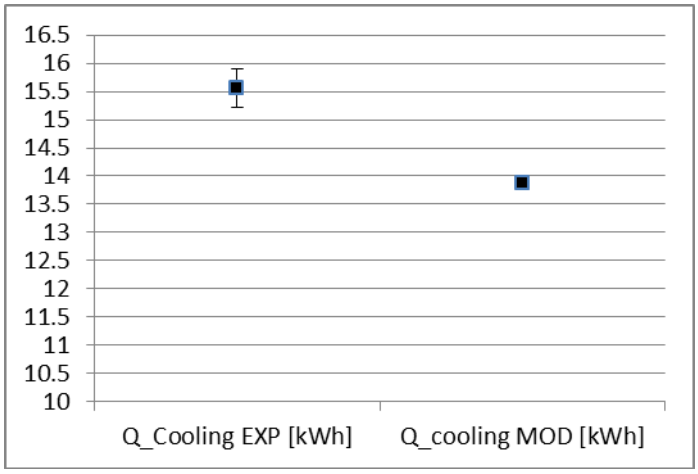

Figure 5.17: Measured and modeled total cooling energy, interior white blind, 45º.

Experiment 5 (E5): Interior blind, white, slats at 90º

The measured daily total cooling energy for the final experimental case was 15.30 kWh. The model predicted a total cooling energy of 15.12 kWh. The peak cooling hour in the model simulation occurs earlier and is lower than was observed in the experimental case. GHR was 7.03 kWh/m2, and the average temperature fort the day was 30.95 ºC.

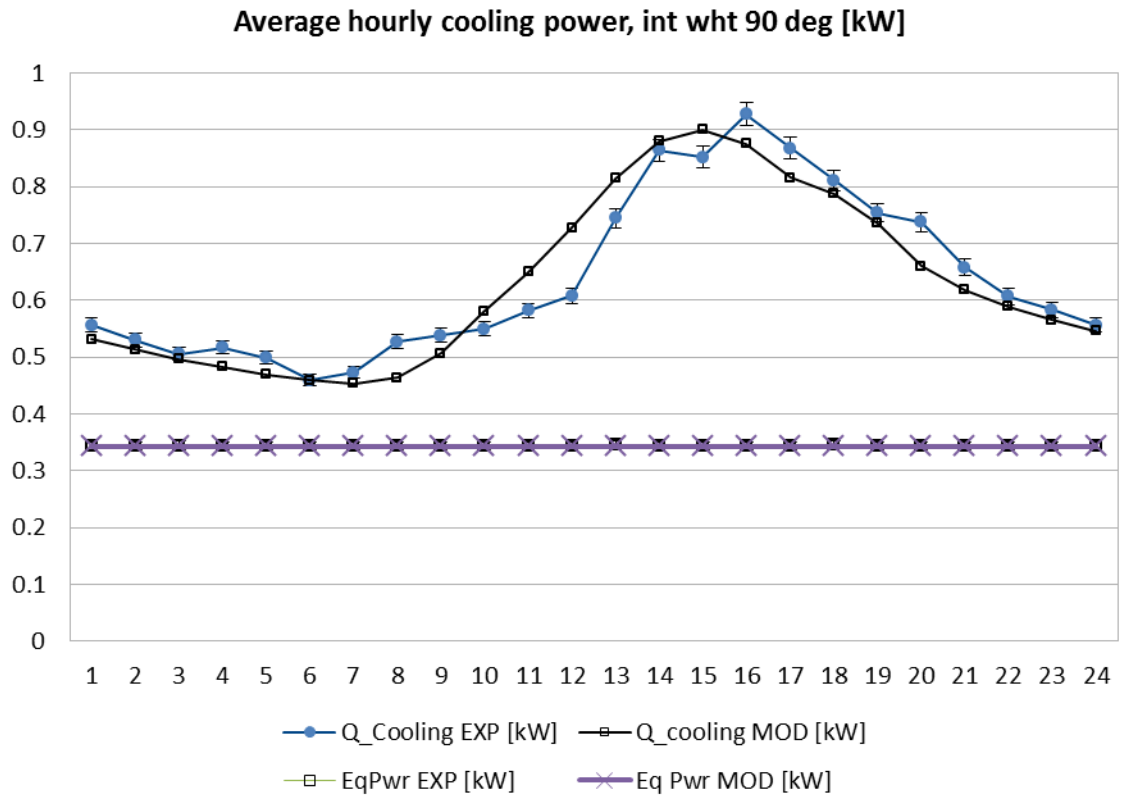

Figure 5.18: Measured and modeled cooling rate, int white blind, 90º.

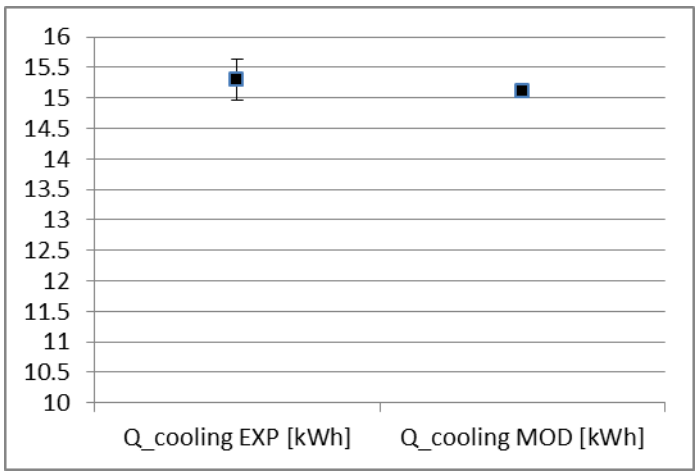

Figure 5.19: Measured and modeled total cooling energy, int white blind, 90º.

ANALYSIS OF EXPERIMENTAL RESULTS

Since weather conditions were different for each experiment a direct comparison of the results must be made with caution. A chart of results not adjusted for weather is shown in Figure 5.19, and a comparison of peak cooling power is shown in Figure 5.20.

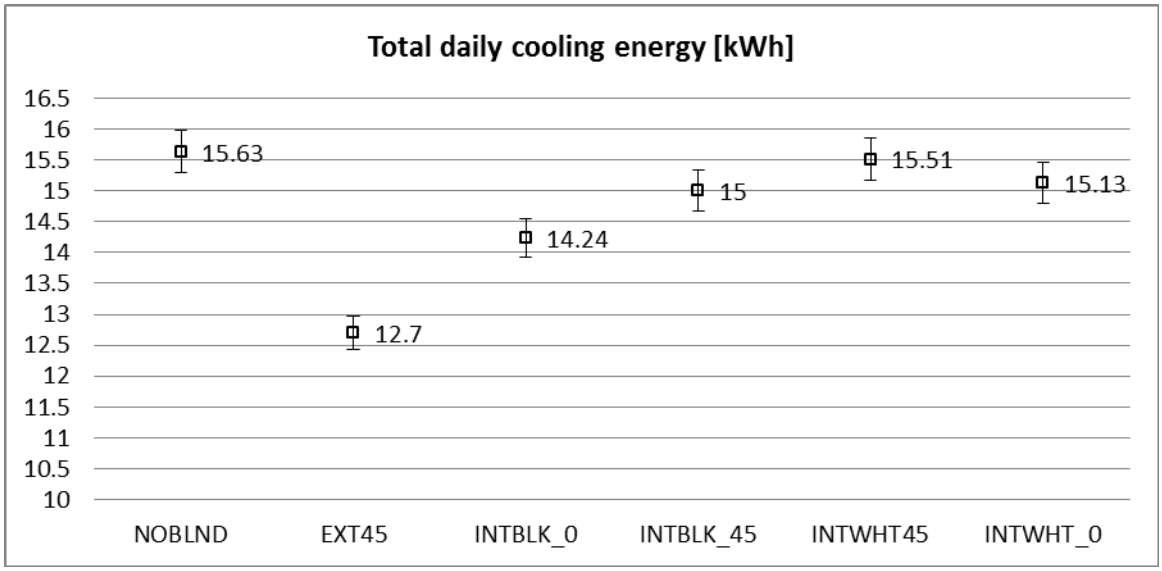

Figure 5.20: Comparison of all experiments, total cooling energy

In this comparison, aspects of the result support certain hypothesis and results of previous research. The experiment with no blind shows the highest cooling consumption, and the lowest cooling energy was exhibited when the exterior blind was deployed. Less energetic than average weather conditions on these testing days may have caused a relatively lower cooling energy when compared to the other experiments. The effect of this would be to reduce the difference between the cooling energy for the no-blind experiment and the other experiments, and to enhance the difference between the external blind case and the other results (cooling energy may be lower in part due to weather). The

results for internal blinds are mixed. In both 45º and 90º configurations, the black blind experiments exhibit lower cooling energy than those using white blinds. Interestingly, the experiments with internal blinds with slats at 45º show higher cooling energy than the same blind type for 90º cases.

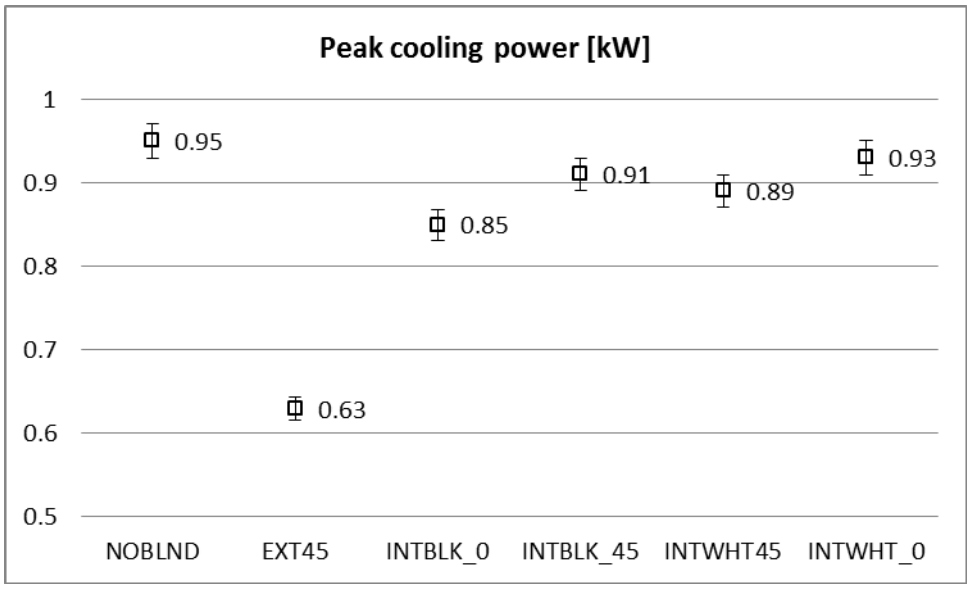

Figure 5.21: Comparison of all experiments, cooling power at peak

The results of peak cooling power show the same relative performance as daily cooling energy with one exception. Whereas the interior white blind at 45º shows the highest energy consumption of any interior blind, the magnitude of its peak hour is lower than both the 45º interior black blind and 90º interior white blind.

EXPERIMENTAL LIMITATIONS

Since the individual experiments were conducted on different days, with different solar and weather conditions, caution must be employed when comparing cooling loads to assess the relative performance of the blinds. An attempt was made in the discussion of

the results to understand the direction, but not precise magnitude, of relative effect of weather between the various experiments. It is also true, however, that weather conditions were very similar in temps of outdoor air temperature for all days, and for solar radiation (GHR) for all but the exterior blind experiment. A second test chamber is currently under construction which will allow parallel testing of two different configurations, and could be used for a follow-up study.

Given the relatively low levels of solar radiation transmitted through the window assembly—especially in the case of blinds—the pyranometer used on the inside of the window assembly has a higher than desirable error of ±10%. The sensor was employed after a more sensitive instrument suffered failure. While the data from the sensor is not used in calculation of the primary cooling energy metric, the imprecision of this measurement makes it difficult to perform a reliable finer-grained analysis of the blind performance in order to determine the components of solar energy transmitted and reflected to the room between the slats, versus the absorbed energy and energy reflected outward.

A second limitation is that incident normal solar radiation on the exterior of the lab's facade was not measured for all days. Again, this data is not used in the measurement of cooling energy, but it could have been used for deeper analysis of the window performance. It would have also served to check for agreement of modeled external incident normal solar radiation calculated within the simulation. This was done for the "calibration experiment" with no blinds, and the model was found to have excellent agreement with the measured value, which gives a measure of confidence that modeled exterior normal incident solar radiation was reasonable for all days.

At the time of the experiments, the precise emissivity of the blinds was not known. Blind material will be sent for testing after this paper is submitted, and the results

will be used in additional future analysis. Knowing the precise values would allow for closer analysis of the influence of the blind in both simulation and experiments.

Ideally, each experiment would have been repeated several times. An unexpectedly long calibration period due to the need for sensor replacements and investigation of data logging errors compressed the time available for repetition and follow-up investigations. Each final experiment lasted 24 hours after which the lab was immediately reconfigured for the next experiment. One concern is that the previous day of experiments influences the starting conditions of the following experiment.

Finally, to make the experiments more applicable to typical concrete high-rise construction, more thermal mass could be added to the floor of the test cell. This was considered, but not done, in part due to concerns over load tolerances on the testing deck. Simulations were performed prior to the start of experiments, using a model different from the more detailed one developed during the study, which predicted only slight overall differences with the addition of a 10 cm concrete block layer. This assumption has not been reexamined with the current version of the model.

LIMITATIONS OF THE SIMULATION MODEL

Built into the simulation model is an assumption that the room air is well-mixed. Goldstein (2009) points out that with a ceiling slot diffuser, the air in the room is gradated; at the diffuser, cold supply air enters the room and washes the window.[6] Since the air jet from the diffuser "attaches" to the window surface due to the coanda effect, the external window is essentially an isolated area from the rest of the space, and so supply air temperature, rather than room temperature is a better input for calculation of overall window surface convection. Thus there may be a mischaracterization of the rate of

[6] Goldstein, Kaitlin Ryan. 2009.

convection from the window/blind assembly to the room as a result of the well-mixed air assumption. Since the rate of convection at the window/blind surfaces is deemed to be a strong factor in the modulation of instantaneous (and peak) cooling power, it is important to accurately capture it in the model. It is not stated in the EnergyPlus engineering documentation if the algorithm attempts to correct the selected convection coefficient model to use room air temperature rather than supply air temperature. This effect will be tested in continuing research, either by assigning a reasonable fixed convection coefficient for the interior side of window assembly, or by using a room air model that captures thermal heterogeneity.

A known shortcoming of the EnergyPlus slat blind model is its failure to account for blind slat curvature. Chantrasrisalai and Fisher (2004) found that this can result in a significant over-prediction of direct-to-direct transmittance through the blind to the room. Improving this aspect of the blind model is a worthy topic for future research.

Finally, the simulation model has not been examined for uncertainty. This analysis will be performed in a future extension of the project.

Chapter 6: Conclusion

This paper examined the effect of various blind configurations on cooling power and energy in an outdoor test chamber that simulates a typical highly glazed cell of a commercial office building. Certain hypotheses appear to be supported by the results. In all cases, blinds reduced cooling energy relative to the experiment with no blinds. The exterior blind experiment exhibited the lowest cooling energy of all the experiments. For both dark and light interior blinds, the cases with slat angles at 45º resulted in higher cooling energy than the open blind case for the same blind color. This may support previous research findings using simulation and small-scale test chambers that found that interior blinds can prevent a portion of incoming solar energy from reaching the thermal mass of room surfaces, and convert the energy to an instantaneous convective load.

Since the individual experiments were conducted on different days, with different solar and weather conditions, caution must be employed when comparing cooling loads to assess the relative performance of the blinds. An attempt was made in the discussion of the results to understand the direction, but not precise magnitude, of relative effect of weather between the various experiments. It is also true, however, that weather conditions were very similar in temps of outdoor air temperature for all days, and for solar radiation (GHR) for all but the exterior blind experiment. A second test chamber is currently under construction which will allow parallel testing of two different configurations, and could be used for a follow-up study.

Acknowledgements

An ASHRAE Grant-in-Aid funded this research.

Bibliography

Barnaby, Charles S., John L. Wright, and Michael R. Collins. 2009. “Improving Load Calculations for Fenestration with Shading Devices.” ASHRAE Transactions 115 (2) (October): 31–44.

Chantrasrisalai, C., and D.E. Fisher. 2004. Comparative Analysis of One-Dimensional Slat-Type Blind Models. Proceedings of the SimBuild 2004 Conference, August 4-6, Boulder, Colorado. BPSA-USA.

Collins, M.R. 2004. Convective Heat Transfer Coefficients from an Internal Window Surface and Adjacent Sunlit Venetian Blind. Energy and Buildings, Vol 36 (3), pp. 309-318.

EnergyPlus Development Team. 2010. *EnergyPlus Engineering Documentation*

Fisher, D. E., and C. O. Pedersen. 1997. “Convective Heat Transfer in Building Energy and Thermal Load Calculations.” *Transactions-ASHRAE* 103: 137–148.

Goldstein, K. and Novoselac, A. (2010) Convective Heat Transfer in Rooms With Ceiling Slot Diffusers (RP-1416). HVAC&R Research Journal, 16 (5), 629-655.

Goldstein, Kaitlin Ryan. 2009. *Convective Heat Transfer in Rooms with Ceiling Slot Diffusers.* Austin, Tex: University of Texas.

Gomes, M. Glória, A. Moret Rodrigues, and J. Alexandre Bogas. 2012. “Numerical and Experimental Study of the Optical Properties of Venetian Blinds.” Journal of Building Physics (May 15). doi:10.1177/1744259112444022. http://jen.sagepub.com.ezproxy.lib.utexas.edu/content/early/2012/05/06/1744259112444022.

Loutzenhiser, Peter G., Heinrich Manz, Sven Moosberger, and Gregory M. Maxwell. 2009. “An Empirical Validation of Window Solar Gain Models and the Associated Interactions.” International Journal of Thermal Sciences 48 (1) (January): 85–95. doi:10.1016/j.ijthermalsci.2008.01.011.

Loutzenhiser, Peter G., Heinrich Manz, Stephan Carl, Hans Simmler, and Gregory M. Maxwell. 2008. “Empirical Validations of Solar Gain Models for a Glazing Unit with Exterior and Interior Blind Assemblies.” Energy and Buildings 40 (3): 330–340. doi:10.1016/j.enbuild.2007.02.034.

Roeleveld, Derek, David Naylor, and Pat Oosthuizen. 2010. “A Simplified Model of Heat Transfer at an Indoor Window Glazing Surface with a Venetian Blind.” Journal of Building Performance Simulation 3 (2): 121–128. doi:10.1080/19401490903528147.

Tzempelikos, Athanassios, and Andreas K. Athienitis. 2007. “The Impact of Shading Design and Control on Building Cooling and Lighting Demand.” Solar Energy 81 (3) (March): 369–382. doi:10.1016/j.solener.2006.06.015.

Wright, John L., Michael R. Collins, Nathan A. Kotey, and Charles S. Barnaby. *Improving cooling load calculations for fenestration with shading devices.* Atlanta, GA: ASHRAE, 2009.

Vita

Greg Arcangeli holds a B.A. in Sociology and French from Georgetown University, and an M.Arch. from the University of Texas at Austin School of Architecture (UTSoA). His recent professional experience includes a position at the architecture firm of Massimiliano Fuksas Architetto in Rome, Italy, and work as a Graduate Engineer for the City of Austin at Austin Energy Green Building.

Email: greg.arc@gmail.com

This thesis was typed by Gregory Nicholas Arcangeli.